Printing nanoparticle building blocks from the gas phase using nanoxerography

Chad R. Barry, Nyein Z. Lwin, Wei Zheng, and Heiko O. Jacobs[a)]
Department of Electrical and Computer Engineering, University of Minnesota, 200 Union Street SE, Minneapolis, Minnesota 55455

(Received 28 July 2003; accepted 15 October 2003)

This letter reports on the electrostatic driven self-assembly of nanoparticles onto charged surface areas (receptors) from the gas phase for nanoparticle based device fabrication. The charged areas were generated by a parallel technique that uses a flexible, conductive electrode to pattern electrons and holes in a thin film electret. Samples, 1 cm^2 in size, were patterned with charge in 10 s with 100 nm scale resolution. Charge based receptors, 100 nm$\times$100 nm in size, contained $\sim$100 elementary charges. A transparent particle assembly module was designed to direct and monitor the assembly of metallic nanoparticles at a resolution of 100 nm, which is $\sim$3 orders of magnitude greater than the resolution of existing xerographic printers. © *2003 American Institute of Physics.*
[DOI: 10.1063/1.1637143]

Nanoparticles are considered the building blocks of future nanotechnological devices. Nanoparticles are typically created in the gas or liquid phase. Silicon nanoparticles generated by silane pyrolysis or electrochemical reaction of hydrogen–fluoride with hydrogen–peroxide are used for nonvolatile memories,[1] lasers,[2] and biological markers.[3] Evaporated gold,[4] indium,[5] and ion sputtered aluminum[6] nanoparticles are used for single electron transistors; and electron beam evaporated gold and silver particles are used for plasmonic waveguides.[7] The use of nanoparticles as building blocks, regardless of the application, requires new assembling strategies. Most actively studied approaches include: (i) single particle manipulation,[8] (ii) random particle deposition,[5] and (iii) parallel particle assembly, based on self-assembly.[9–16]

The use of high resolution charge patterns to direct the assembly of nanoparticles was first proposed by Wright and Chetwynd in 1998.[14] Since then, several serial charge-patterning processes have been explored to enable the positioning of nanoparticles.[15,17–19] Serial techniques, however, remain slow—the fastest scanning probe-based system needs 1.5 days to pattern an area of 1 cm^2.[20] As a new direction, we have developed a parallel charge patterning process[16] enabling nanoxerographic printing.[21] The printing technique, referred to as electric nanocontact printing, generates a charge pattern based on the same physical principles used in scanning probes but forms multiple electric nanocontacts of different size and shape to transfer charge in a single step. With this method, we demonstrated patterning of charge with 100 nm scale resolution and transfer of 50 nm to 20 μm sized particles including iron oxide, graphitized carbon, iron beads, and Xerox toner from a powder, gas, and liquid phase.[16,21] Others that adopted our technique have also demonstrated the assembly of gold nanoparticles from an aerosol.[22]

In this letter we demonstrate charge patterning using flexible thin silicon electrodes and nanoxerographic printing of 10–200 nm sized metallic nanoparticles. The resolution of this nanoxerographic process is 100 nm, which is $\sim$1000 times higher than the resolution accomplished using traditional xerographic printers,[23,24] and 5 times higher than our previously reported results.[21]

The electric nanocontact printing process to generate charge patterns is illustrated in Fig. 1. In our experiments we tested two different flexible electrodes to accomplish charge transfer. The first electrode prototype was made out of a 5 mm thick poly-(dimethylsiloxane) (PDMS) stamp that was fabricated from a silicon mold defined by e-beam lithography.[25] The second electrode prototype was made from a 2 in. in diameter, 10 μm thick, n-doped silicon wafer (Virginia Semiconductors) patterned by phase-shift lithography[26] and etching in a 98% CF_6, 2% O_2 plasma and supported on a Au coated flat slab of PDMS. The electrodes carried a topographical relief pattern including 100–300 nm wide lines and rings that were $\sim$300 and 150 nm deep, respectively. The PDMS stamp was coated with a 60 nm thick layer of gold by thermal evaporation to provide electrical conductivity. The thin silicon electrode is sufficiently conductive and does not require a metal coating. As charge storage medium we used a 60 nm thick film of PMMA on ⟨100⟩ silicon wafers with a resistivity of 3 Ω cm. The film was formed by spin coating a 2% solution of 950 K (PMMA) in

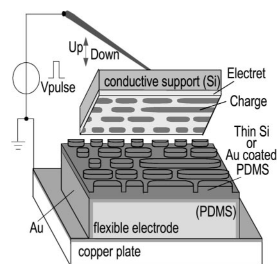

FIG. 1. Principle of parallel charge patterning: A silicon chip carrying a thin film electret is placed on top of a flexible electrode supported by PDMS on a copper plate. A needle, attached to a micromanipulator is used to form an electric contact to the backside of the silicon chip. An external voltage is used to transfer a pattern of charge into the electret material at the areas of contact. The silicon chip is removed with the electret carrying a charge pattern.

[a)]Author to whom correspondence should be addressed; electronic mail: hjacobs@ece.umn.edu

 © 2003 American Institute of Physics
Downloaded 30 Dec 2003 to 128.101.170.38. Redistribution subject to AIP license or copyright, see http://ojps.aip.org/aplo/aplcr.jsp

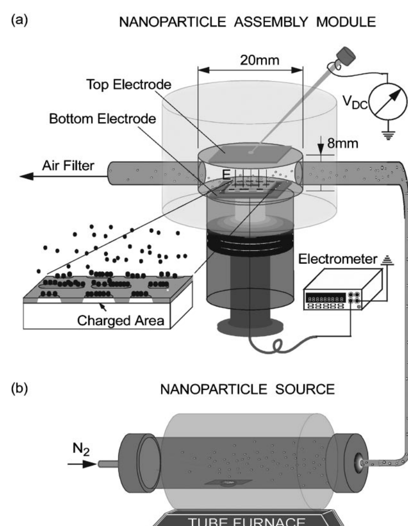

FIG. 2. Principle of nanoxerographic printing from the gas phase. (a) The directed assembly of the nanoparticles occurs in the particle assembly module. An external potential, V_{dc}, applied to the top electode directs incoming nanoparticles to the charged sample surface. The electrometer measures the amount of assembled, charged particles during the assembly process. (b) A constant flow of nanoparticles is generated by evaporation of matter in the tube furnace, transport of the atoms to the outlet by the N_2 gas, and condensation.

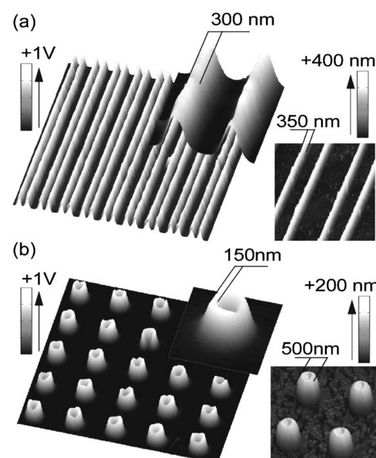

FIG. 3. Kelvin probe force microscopy images of patterns of positive charge (left) in PMMA and corresponding atomic force microscope images of the topography of the electrode structures (right) used to generate the charge patterns: (a) surface potential image of 300 nm (FWHM) positively charged parallel lines generated using a thin silicon electrode; (b) surface potential image of 150 nm wide positively charged rings generated using a PDMS electrode.

chlorobenzene (MicroChem Co.) at 5000 rpm and baking it in an oven at 90 °C for 1 h. The chips were placed on the flexible electrode by hand and contacted from the back with a metallic needle attached to a micromanipulator. To generate a pattern of trapped charge, we applied an external potential for 10 s. During the exposure, we monitored the current flow and adjusted the voltage (5–20 V) to get an exposure current of 0.1–1 mA. After exposure, we removed and characterized the charge patterns using Kelvin probe force microscopy (KFM).[27,28]

The nanoxerographic process to direct the assembly of nanoparticles from the gas phase is illustrated in Fig. 2. The primary unit [Fig. 2(a)], referred to as the particle assembly module, consists of a cavity that holds the sample, two electrodes to generate a global electric field that directs incoming charged particles towards the sample surface, and an electrometer to count the charge of the assembled particles. This module is attached to a tube furnace [Fig. 2(b)] that generates the nanoparticles by evaporation and condensation. For details on the fabrication of this module we refer to EPAPS Ref. 29. To direct the assembly of incoming charged particles we integrated two electrodes into the transparent assembly module. A 2 cm long and 1 cm wide electrode located at the top of the cavity and a 1.5 cm by 1 cm wide electrode underneath the sample. During operation, the electrodes are spaced by ~7 mm and we apply an external voltage of up to ±1000 V to bring charged particles of one polarity into the proximity of the charged sample surface. To monitor the amount of particles that assembled onto the sample under different assembly conditions we implemented a Faraday cup in the assembly module. In our Faraday cup arrangement, the sample forms the cup electrode and is connected to ground with the electrometer (Keithley 6517A) in between. During assembly, image charges flow from the ground through the electrometer into the sample to the location of assembled, charged particles. As a result, the electrometer measures the accumulated charge of the assembled particles.

The particles were generated in a tube furnace. The material to be evaporated is placed inside the quartz tube at the center of the furnace. Pure nitrogen is the carrier gas that flows through the system during operation. The evaporation was carried out at 1100 °C for gold and silver, and 1000 °C for indium. A vapor containing atoms of the evaporated material forms within the furnace. The nitrogen carrier gas transports the atoms out of the furnace where they nucleate and condense into particles due to the change in temperature. The gas flow carries the nanoparticles into the particle assembly module through a 1-m-long Tygon tube.

Representative patterns of localized charge in PMMA recorded by KFM are illustrated in Fig. 3. Figure 3(a) shows the surface potential for a surface that was patterned with 300 nm (FWHM) wide parallel lines using a thin silicon electrode. Figure 3(b) shows 150 nm wide ring patterns generated with a PDMS electrode structure that had a recessed center of 20 nm. This demonstrates that high aspect ratio electrode structures are not required for pattern transfer. Pattern transfer occurs only at the contact areas. Both charge patterns were written by exposing the PMMA film locally with a current density of 1 mA/cm^2 for 10 s with the electrode positive. The recorded surface potential is proportional to the density of trapped charges. For the recorded potential difference we estimated that a 100 nm × 100 nm sized receptor contains 100 elementary charges. For details of this estimate, we refer to EPAPS Ref. 29.

These charge patterns attract nanoparticles. Figure 4 shows representative images of nanoxerographic printing onto these charge patterns. The images show patterns of gold [Fig. 4(a)], silver [Figs. 4(b) and 4(c)], and indium [Figs. 4(d) and 4(e)] nanoparticles that assembled on positively and negatively charged areas from the gas phase. The resolution achieved is 100 nm for the silver and indium particles and 200 nm for the gold nanoparticles.

The electrometer reading and the global electric field are

Downloaded 30 Dec 2003 to 128.101.170.38. Redistribution subject to AIP license or copyright, see http://ojps.aip.org/aplo/aplcr.jsp

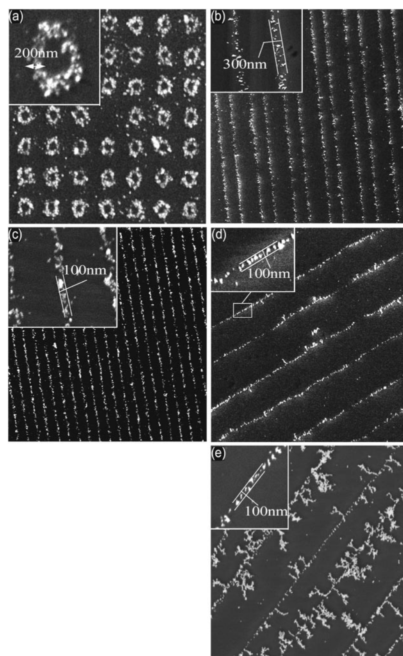

FIG. 4. SEM images of different nanoparticle assemblies. Images (a),(c) were patterned using PDMS electrodes, while images (b),(d),(e) were patterned with thin silicon electrodes: (a) gold nanoparticles assembled onto negatively charged 200 nm wide rings; (b),(c) silver nanoparticles assembled onto positively charged 300 and 100 nm wide lines; (d),(e) indium nanoparticles assembled onto positively charged 100 nm wide lines. Image (e) shows dendrite formation of indium that occurs for extended assembly periods.

two important parameters to control the assembly process, the coverage, the particle polarity that assembles on the surface, and the speed of the assembly. We observed a clear proportionality between the electrometer reading and the coverage. Excellent coverage and high selectivity were obtained when ± 4 nC of charged silver particles or ± 1 nC of charged indium particles accumulated on the sample, whereas at ± 10 nC the sample would be fully coated. The global electric field controls the polarity of assembled particles. Nanoparticles assembled well on positively charged areas [Figs. 4(b)–4(e)] by applying a negative potential to the top electrode, whereas for negatively charged areas [Fig. 4(a)] a positive potential was required. The global electric field also effected how fast the assembly took place. At ± 1 kV and 1100 °C, the assembly time to get good coverage for silver at a flow rate of 1000 ccm was 1 min whereas at ± 100 V it took 10 min to get the same coverage. The assembly of the indium particles took place at a higher deposition rate than the silver particles. This could possibly be explained by the higher vapor pressure of indium at the noted evaporation temperatures. The assembly time was 20 s at -1 kV and 2 min at -100 V. For longer assembly times of indium, we found the formation of dendrites that grew perpendicular to the field lines [Fig. 4(e)].

In this letter, we demonstrated nanoxerographic printing with 100 nm resolution. The resolution of the developed technique is currently limited by the smallest possible feature size on the electrode structure. For the PDMS based electrode structure this limit is ~ 100 nm. Smaller features tend to collapse. Higher resolution might become possible using the proposed thin silicon, which is capable of supporting ~ 10 nm sized features.[30] The first results of nanoxerographic printing using the thin silicon are very encouraging. Whether nanoxerography will enable the printing of nanoparticle based devices remains to be shown. However, nanoxerography offers a very competitive strategy compared to other techniques. It can handle all kinds of materials, is parallel, and could potentially accomplish 10 nm scale resolution or better.

Financial support from the National Science Foundation (DMI-0217538, ECS-0229087, and IGERT) is kindly acknowledged.

[1] M. L. Ostraat, J. W. De Blauwe, M. L. Green, L. D. Bell, M. L. Brongersma, J. Casperson, R. C. Flagan, and H. A. Atwater, Appl. Phys. Lett. **79**, 433 (2001).
[2] M. H. Nayfeh, S. Rao, N. Barry, J. Therrien, G. Belomoin, A. Smith, and S. Chaieb, Appl. Phys. Lett. **80**, 121 (2002).
[3] G. Belomoin, J. Therrien, A. Smith, S. Rao, R. Twesten, S. Chaieb, M. H. Nayfeh, L. Wagner, and L. Mitas, Appl. Phys. Lett. **80**, 841 (2002).
[4] C. Thelander, M. H. Magnusson, K. Deppert, L. Samuelson, P. R. Poulsen, J. Nygard, and J. Borggreen, Appl. Phys. Lett. **79**, 2106 (2001).
[5] T. Junno, M. H. Magnusson, S.-B. Carlsson, K. Deppert, J.-O. Malm, L. Montelius, and L. Samuelson, Microelectron. Eng. **47**, 179 (1999).
[6] T. W. Kim, D. C. Choo, J. H. Shim, and S. O. Kang, Appl. Phys. Lett. **80**, 2168 (2002).
[7] S. A. Maier, M. L. Brongersma, P. G. Kik, S. Meltzer, A. A. G. Requicha, and H. A. Atwater, Adv. Mater. (Weinheim, Ger.) **13**, 1501 (2001).
[8] C. Baur, A. Bugacov, B. E. Koel, A. Madhukar, N. Montoya, T. R. Ramachandran, A. A. G. Requicha, R. Resch, and P. Will, Nanotechnology **9**, 360 (1998).
[9] W. A. Lopes and H. M. Jaeger, Nature (London) **414**, 735 (2001).
[10] J. Janin, Prog. Biophys. Mol. Biol. **64**, 2 (1995).
[11] C. M. Niemeyer, B. Ceyhan, S. Gao, L. Chi, S. Peschel, and U. Simon, Colloid Polym. Sci. **279**, 68 (2001).
[12] P. D. Yang, A. H. Rizvi, B. Messer, B. F. Chmelka, G. M. Whitesides, and G. D. Stucky, Adv. Mater. (Weinheim, Ger.) **13**, 427 (2001).
[13] C. Petit, A. Taleb, and M. P. Pileni, Adv. Mater. (Weinheim, Ger.) **10**, 259 (1998).
[14] W. M. D. Wright and D. G. Chetwynd, Nanotechnology **9**, 133 (1998).
[15] H. O. Jacobs and A. Stemmer, Surf. Interface Anal. **27**, 361 (1999).
[16] H. O. Jacobs and G. M. Whitesides, Science **291**, 1763 (2001).
[17] T. J. Krinke, H. Fissan, K. Deppert, M. H. Magnusson, and L. Samuelson, Appl. Phys. Lett. **78**, 3708 (2001).
[18] H. Fudouzi, M. Kobayashi, and N. Shinya, Mater. Res. Soc. Symp. Proc. **636**, D9.8/1 (2001).
[19] P. Mesquida and A. Stemmer, Microelectron. Eng. **61-62**, 671 (2002).
[20] A. Born and R. Wiesendanger, Appl. Phys. A: Mater. Sci. Process. **68**, 131 (1999).
[21] H. O. Jacobs, S. A. Campbell, and M. G. Steward, Adv. Mater. (Weinheim, Ger.) **14**, 1553 (2002).
[22] T. J. Krinke, K. Deppert, M. H. Magnusson, and H. Fissan, Part. Part. Syst. Charact. **19**, 321 (2002).
[23] R. Groff, P. Khargonekar, D. Koditschek, T. Thieret, and L. K. Mestha, Proceedings of the 38th IEEE Conference on Decision and Control 2 (1999).
[24] D. M. Pai and B. E. Springett, Rev. Mod. Phys. **65**, 163 (1993).
[25] Y. Xia and G. M. Whitesides, Angew. Chem., Int. Ed. Engl. **37**, 550 (1998).
[26] T. W. Odom, J. C. Love, D. B. Wolfe, K. E. Paul, and G. M. Whitesides, Langmuir **18**, 5314 (2002).
[27] H. O. Jacobs, H. F. Knapp, S. Muller, and A. Stemmer, Ultramicroscopy **69**, 39 (1997).
[28] H. O. Jacobs, P. Leuchtmann, O. J. Homan, and A. Stemmer, J. Appl. Phys. **84**, 1168 (1998).
[29] See EPAPS Document No. E-APPLAB-83-011352 for details on the fabrication of the particle assembly module and an estimate of the trapped charge density. A direct link to this document may be found in the online article's HTML reference section. The document may also be reached via the EPAPS homepage (http: //www.aip.org/pubservs/epaps.html) or from ftp.aip.org in the directory /epaps/. See the EPAPS homepage for more information.
[30] S. Y. Chou, C. Keimel, and J. Gu, Nature (London) **417**, 835 (2002).

Downloaded 30 Dec 2003 to 128.101.170.38. Redistribution subject to AIP license or copyright, see http://ojps.aip.org/aplo/aplcr.jsp